Available online at www.sciencedirect.com
SCIENCE DIRECT®
Nuclear Physics B (Proc. Suppl.) 136 (2004) 407–414
NUCLEAR PHYSICS B PROCEEDINGS SUPPLEMENTS
www.elsevierphysics.com

Auger FD: Detector Response to Simulated Showers and Real Event Topologies

L. Perrone[a] for the Pierre Auger Collaboration[b]

[a] Bergische Universität Wuppertal, Fachbereich C, Sektion Physik - D-42097 Wuppertal, Germany

[b] Observatorio Pierre Auger, Av. San Martín Norte 304, (5613) Malargüe, Argentina

The performance of the Auger Fluorescence telescope is discussed on the basis of a mass production chain. In order to get a realistic estimate of the detector resolution, a large number of fully simulated CORSIKA [1] showers have been used for this study. The propagation through the atmosphere and the detector response are taken into account and simulated in detail. Results for the the case of monocular reconstruction are presented here. No quality cuts for the event reconstruction have been applied so far. Finally, a schematic overview of the expected event topologies is given together with the display of a real event recently collected.

1. Introduction

The Pierre Auger Cosmic Ray Observatory has been designed to investigate the origin and the nature of Ultra High Energy Cosmic Rays using a hybrid detection technique. Two sites of about 3000 km^2 each, in the northern and in the southern hemispheres, will be equipped with a surface detector (SD) and a set of fluorescence detectors (FD). Each fluorescence detector (eye) consists of 6 mirrors, each with a field of view of $30^\circ \times 30^\circ$. The general design of the experiment has been recently described in [2]. An advanced detector production phase is in progress at the southern hemisphere site (Malargüe, Argentina). SD modules covering a constantly increasing area, at present about 1/4 of that planned, are viewed by two fully operating FD telescopes (up to 4 in the near future). Details on the current status of the project can be found in [3] and in [4] for FD and SD, respectively.

An accurate knowledge of the detector response is essential in order to perform a reliable data analysis. First of all, the concept of simulation and reconstruction for a fluorescence detector is briefly overviewed. Then, the performance of the monocular FD reconstruction is discussed for a large number of CORSIKA simulated showers. The trigger efficiency and the performance of geometry and energy reconstruction are discussed as a function of core distance (shower landing point) and primary energy. The reconstruction of the mass sensitive parameter X_{max} (atmospheric depth at shower maximum) is checked and compared for proton and iron primaries. Finally, the main expected real event topologies are briefly described.

2. Simulation and Reconstruction Concept

In order to identify the quantities playing a key role in a mass production chain for a fluorescence detector, a simplified flow of the simulation-reconstruction concept is briefly described. The number of fluorescence photons N_γ generated by a number of charge particles N_{ch}, propagating through the atmosphere, is given by:

$$N_\gamma = N_{ch} \times Yield_{fl} \times \Delta l \times A/4\pi r^2 \times T_{atm} \quad (1)$$

$$N_{FADC} = \alpha_{cal} \times N_\gamma \quad (2)$$

where:

- $Yield_{fl}$ is the number of fluorescence photons per unit length and per charge particle ($\sim$ 4 photons/m)
- Δl is the path traveled by a single charge particle within a certain observation time-

0920-5632/$ – see front matter © 2004 Elsevier B.V. All rights reserved.
doi:10.1016/j.nuclphysbps.2004.10.044

window (in the case of a vertical shower $\sim$ 30 m for a 100 ns time-bin)

- A is the mirror effective area
- T_{atm} is a coefficient that takes into account the atmospheric attenuation (Rayleigh scattering and Mie scattering)
- r is the distance of the shower track slice to the telescope
- N_{FADC} and α_{cal} are the FACD counts and the detector calibration constants respectively.

For a certain shower geometry and a given landing point, starting either from an analytical or a fully simulated longitudinal profile (number of charge particles as a function of slant depth), the simulation reproduces the FADC traces, taking into account the absorption of the atmosphere and the detector response (leftwards flow in eq. 1 and 2). The reconstruction performs these steps in reverse order. Firstly, the geometry of the shower is determined in two steps. Based on the measured FADC traces, the shower detector plane is calculated. Then, the inclination of the shower axis in this plane is derived from the time sequence of the measured signals. Once the geometry is known, the longitudinal profile is reconstructed taking into account the absorption of the atmosphere (rightwards flow in eq. 1 and 2). The energy estimation is performed by fitting the longitudinal profile and by integrating the resulting function. Corrections for the forward emitted Cherenkov contribution and for the "unseen" energy carried out by neutrinos, high energy muons and nuclear excitations are then applied. Further details on the described method are given in [5–7].

3. The simulation samples

In order to obtain a sufficient number of events the CORSIKA showers have been taken from the large shower database developed in the Lyon computing center for simulation studies with the Auger detector. In particular, two different shower settings have been used which differ in the distribution of the energy and the zenith angle:

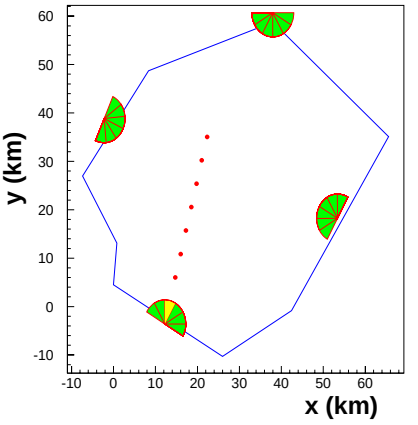

Figure 1. Core locations chosen for the simulation: middle of Bay4 starting at 10 km away from the eye, receding in step of 5 km up to 40 km.

- sample V consists of 800 vertical showers, with discrete energy in a range between $10^{17.5}$ and 10^{21} eV (100 showers per each energy half decade).
- sample D-low consists of showers with energy distributed over a range between 10^{18} and 10^{21} eV according to a power-law with differential index of -2. The zenith angles are distributed between 0° and 60° according to $dN \propto sin\theta\, cos\theta\, d\theta$.

Although setting D-low seems to be much more appropriate for testing the reconstruction chain, due to the spectral feature, it suffers from lack of statistics at high energy. Therefore, the constant number of showers with discrete energies in setting V is complementary to achieve a sufficient number of events for high-energy primaries.
The CORSIKA showers have been simulated in the center of Bay4 (Los Leones eye), with the core location increasing in steps of 5 km, starting at 10 km away from the bay (see Fig. 1). Assumptions for the atmosphere, detector calibration and fluorescence yield calculation have been chosen consistently throughout the simulation-reconstruction chain.

4. Trigger Efficiency

Since sample V contains a wide range of energies and shows no geometric variation, it is the appropriate tool to estimate the trigger efficiency of the detector simulation, as a function of shower core distance, for different energies.

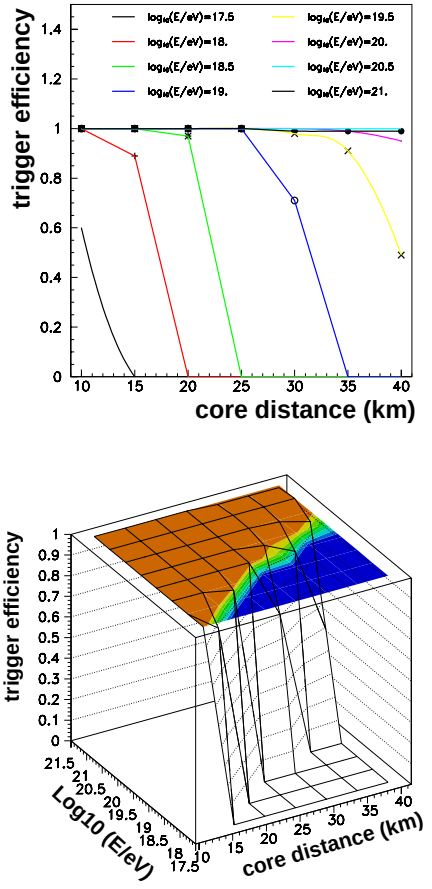

Figure 2. Top panel: trigger rate as a function of core distance for different energies. Bottom panel: differential plot as a function of energy and core distance. Plots are given for sample V.

The top panel of Fig. 2 shows the trigger rate as a function of increasing distance (different colors are for different energies): the higher the shower energy is, the further from the detector that the trigger rates falls off. For example, the trigger efficiency is 100% up to a core distance of 25-30 km for an energy of 10^{19} eV. The bottom panel of Fig. 2 shows a differential plot of the trigger rate as a function of energy and core distance.

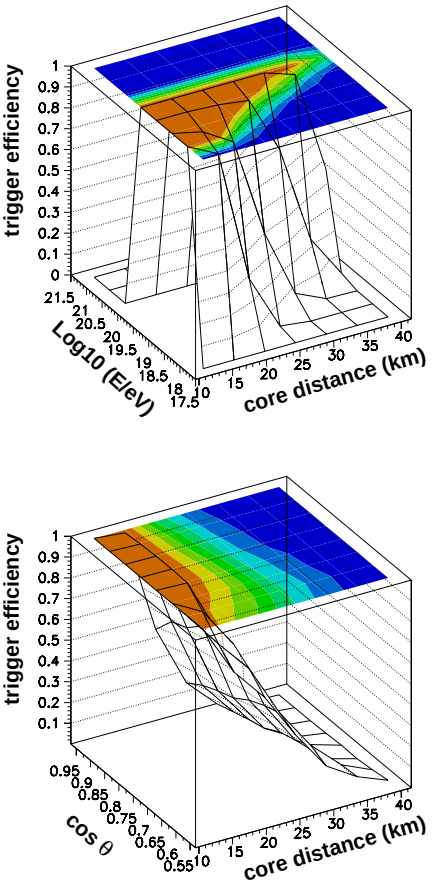

Figure 3. Differential plots with the contribution of individual energies (top panel) and zenith angles (bottom panel). Plots are given for sample D-low.

A much stronger decrease of the overall trigger rates is expected for sample D-low since the shower energies are distributed approximately ac-

cording to a power law with a differential index of -2. In order to show the dependence on the energy and on core distance, a differential plot of trigger rate for sample D-low is given in the top panel of Fig. 3. Finally, as shown in the bottom panel of Fig. 3, the trigger rate is only weakly dependent on the zenith angle for the considered range, i.e. up to 60°.

5. Geometry Reconstruction and Energy Estimate

Fig. 4 shows the resolution of core position (x-coordinate - see Fig. 1) for sample V. Mean values (top panel) and sigmas (bottom panel) of the Gaussian fit to the distribution of $x_{true} - x_{rec}$ are shown as a function of core distance. The accuracy of the reconstruction stays within few hundreds of meters up to a distance of less then 25 km. At larger distances, it becomes poorer due to the attenuation of light in the atmosphere. Fig. 5 shows the zenith angle resolution at a core distance of 10 km for sample D-low. The arrows indicate the FWHM of the $\theta_{true} - \theta_{rec}$ distribution. As shown in Fig. 5, the FWHM is at the level of 1°.

Fig. 6 shows the energy resolution at a core distance of 10 km for sample V (top panel) and for sample D-low (bottom panel). The arrows indicate the FWHM of the $Log_{10}(E_{true}/E_{rec})$ distribution. As shown in Fig. 6, the FWHM are at the level of 6% and 11% for sample V and for sample D-low, respectively. A systematic shift of the reconstructed energies (from 10% up to 15%) is also observed, likely due to unexpected differences of the atmosphere (and/or the fluorescence yield) treatment throughout the simulation-reconstruction chain.

6. X_{max} Reconstruction

Fig. 7 shows the resolution of X_{max} (the atmospheric depth at shower maximum) as a function of core distance for sample V. Mean values and sigmas of the $X^{true}_{max} - X^{rec}_{max}$ distribution are given in the left and in the right panel of Fig. 7, respectively.

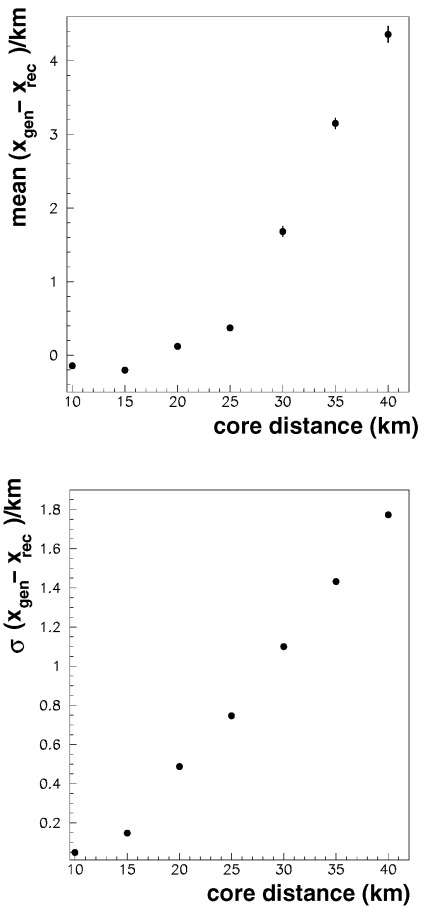

Figure 4. Resolution of core position (x-coordinate) for sample V. Mean values (top) and sigmas (bottom) of the Gaussian fit to the distribution of $x_{true} - x_{rec}$ are shown as a function of core distance.

7. Proton and Iron comparison

In the frame of mass separation studies, the X_{max} resolution has been calculated for proton and iron primaries separately. Fig. 8 shows the resolution of X_{max} as a function of core distance for the sample D-low. Mean values and sigmas of the $X^{true}_{max} - X^{rec}_{max}$ distribution are given in the top and in the bottom panel for proton (black points)

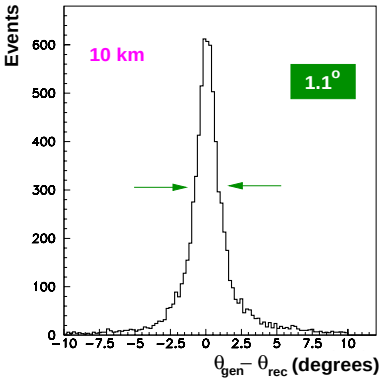

Figure 5. Zenith angle resolution at a core distance of 10 km for sample D-low. The arrows indicate the FWHM (1.1°) of the distribution.

Table 1: Mean values and sigmas of the generated and reconstructed X_{max} distributions for proton and iron primaries (sample D-low at a core distance of 15 km).

	Mean (g/cm^2)	Sigma (g/cm^2)
Proton (rec)	759	80
Proton (gen)	733	50
Iron (rec)	674	53
Iron (gen)	651	25

and for iron (red points) primaries. The X_{max} resolution for iron primaries remains slightly better than for protons over the full range of core distances. This is as expected, since fluctuations of first interaction are smaller for heavier nuclei. Fig. 9 shows the generated (solid line) and the reconstructed (dashed line) X_{max} distribution for proton (black) and iron (red) primaries at a core distance of 15 km (sample D-low). The distributions are superimposed and compared. As shown in Table 1, the broadening introduced by the detector response results in an an additional spread of about 30 g/cm^2 only weakly depending on the primary mass.

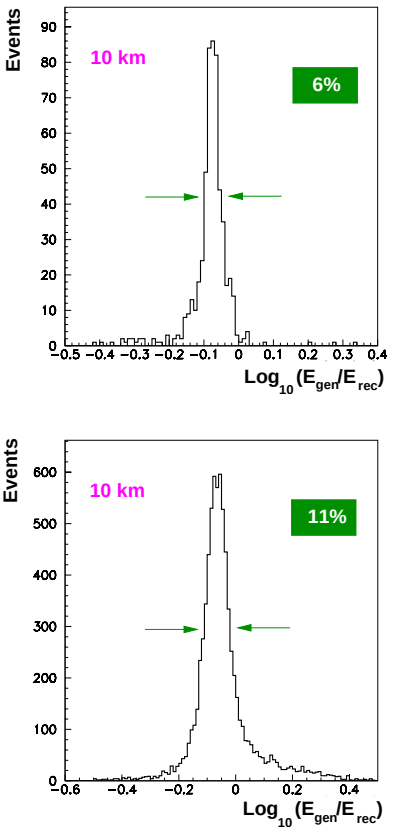

Figure 6. Energy resolution at a core distance of 10 km for sample V (top panel) and for sample D-low (bottom panel). The arrows indicate the FWHM (6% and 11%, respectively) of the distribution.

8. Real Event Topologies

A schematic description of the expected real event topologies is given below:

- *Mono*: at least 1 mirror in any eye
- *Multi-mirror*: at least 2 adjacent mirrors in any eye
- *Stereo*: at least 2 mirrors in 2 different eyes
- *Hybrid*: at least 1 mirror in any eye in coincidence with a signal from SD

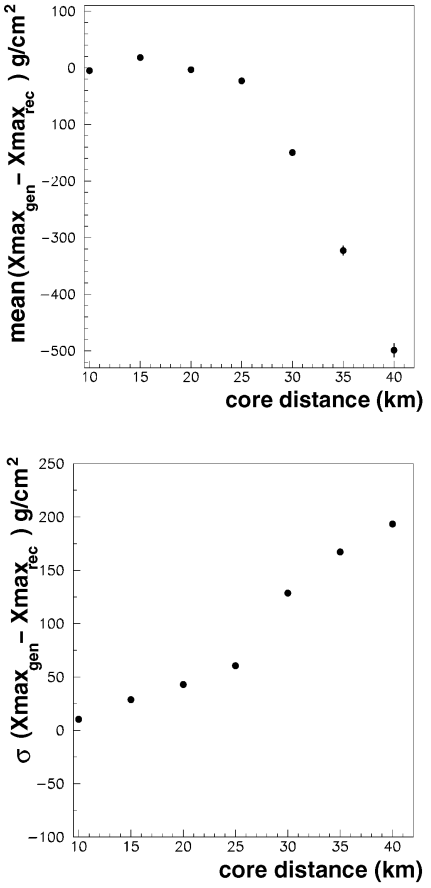

Figure 7. X_{max} resolution for sample V. Mean values (up) and sigmas (down) of the Gaussian fit to the $X_{max}^{true} - X_{max}^{rec}$ distribution are shown as a function of core distance.

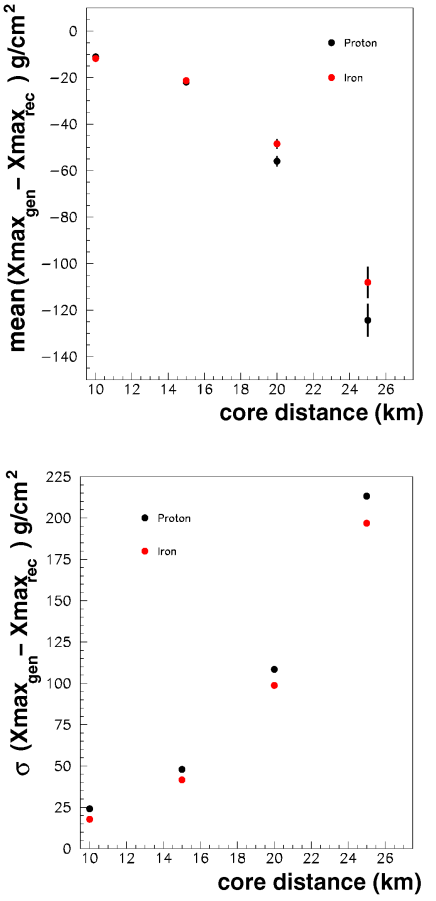

Figure 8. X_{max} resolution as a function of core distance for sample D-low. Mean values and sigmas of the Gaussian fit to the distribution $X_{max}^{true} - X_{max}^{rec}$ are given in the top and in the bottom panel for proton (black points) and for iron (red points) primaries, respectively.

- *Stereo-Hybrid*: at least 2 mirrors in 2 different eyes in coincidence with a signal from SD (see Fig. 10 for a graphical description of this topology).

The SD and FD displays of a real stereo-hybrid event are shown in Fig. 11. For this event, geometry and energy reconstruction from SD and FD agree well. The longitudinal profile from FD is also shown. Results are very preliminary but highly encouraging. A combined hybrid (SD and FD) analysis will improve the global quality of the reconstruction and allow cross calibration of both systems.

9. Conclusions

The performance of the Auger FD monocular reconstruction has been discussed using a large

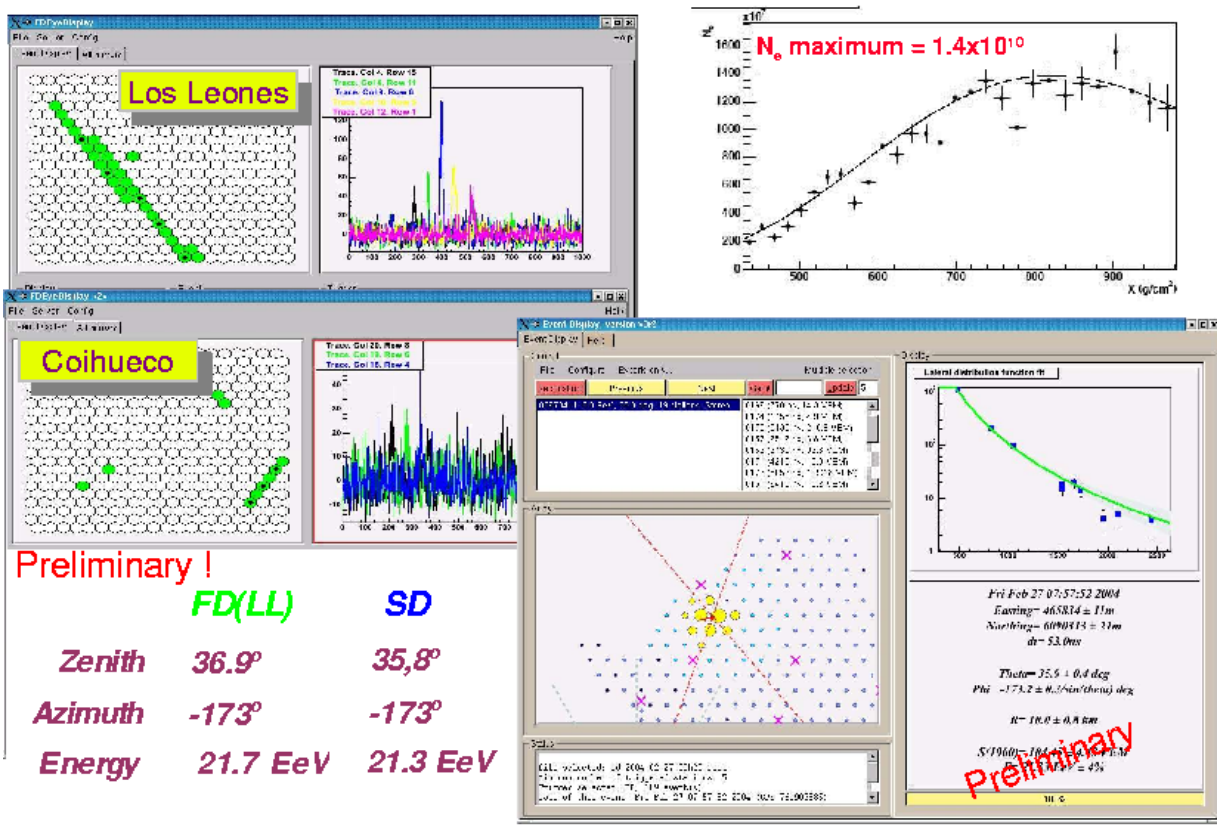

Figure 11. SD (bottom-right) and FD (top-left) displays of a real stereo-hybrid event collected on Feb 27th 2004. The reconstructed profile from FD (Los Leones) is shown on the top-right. SD and FD results are summarized on the bottom-left. All results are very preliminary.

Table 2: Performance of the Auger FD *monocular* reconstruction at a core distance of 10 and 20 km for sample V and sample D-low. No quality cuts applied so far; only statistical fluctuations are included.

	Resolution (sample V)		Resolution (sample D-low)	
	10 km	*20 km*	*10 km*	*20 km*
Zenith	1°	2°	1°	2°
R	100 m	900 m	300 m	5000 m
X_{max}	15 g/cm^2	50 g/cm^2	25 g/cm^2	110 g/cm^2
Energy	6%	10%	11%	23%

number of CORSIKA simulated showers (no quality cuts have been applied so far). Results are summarized in Table 2 for sample V and for sample D-low. Geometry reconstruction works well up to 25 (15) km away from the eye for vertical (distributed) showers. The energy resolution (statistical fluctuation only) remains below 10% up to 25 km away from the eye for vertical

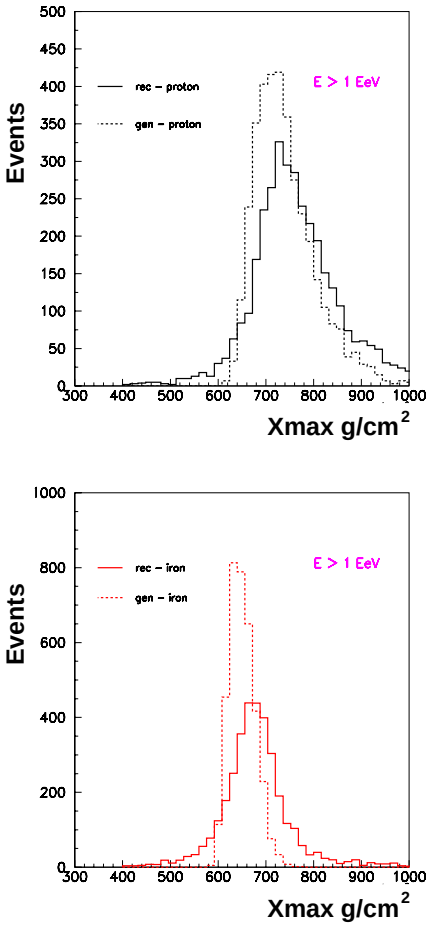

Figure 9. Reconstructed (solid line) and generated (dashed line) X_{max} distribution at 15 km core distance, for sample D-low. The proton case (black line) is shown in the top panel, the iron case (red line) is shown on the bottom panel

showers ($10^{18} < E < 10^{20}$ eV). The achieved values fulfill our expectation. Stereo and/or hybrid detection will highly improve the quality of the reconstruction. Finally, the event topologies have been described and a real stereo-hybrid event was displayed. The technical performance of the detector for the different topologies is fully satisfactory.

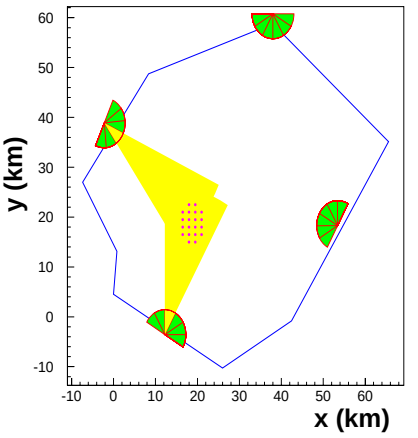

Figure 10. Sketch view of the Stereo-Hybrid topology: at least 2 mirrors in 2 different eyes in coincidence with a signal from SD.

The group of University Wuppertal is supported by the German Ministry for Research and Education (Grant 05 CU1VK1/9)

REFERENCES

1. D. Heck et al. *CORSIKA Cosmic Ray Simulation for Kascade*, Report FZKA 6019, (1998).
2. J. Abraham et al. Nucl. Instr. & Methods A , 523 (2004) 50
3. P. Privitera for the Auger Collaboration, *The Fluorescence Detector of Pierre Auger Observatory*, at this Conference
4. T. Suomijarvi for the Auger Collaboration *"Pierre Auger Observatory: Surface detector"*, at this Conference
5. C.Song et al., Astrop. Phys. 14 (2000) 7.
6. S. Argiro for the Auger Collaboration, Proc of 28th Int. Cosmic Ray Conf. ICRC 2003, Tsukuba, Japan
7. P. Privitera for the Auger Collaboration Proc of 28th Int. Cosmic Ray Conf. ICRC 2003, Tsukuba, Japan